Energy loss of fragment protons dissociated from 0.2- and 0.5-MeV/amu H_2^+ ions incident in carbon foils

Yasufumi Susuki,* Martin Fritz,† Kenji Kimura, and Michi-hiko Mannami
Department of Engineering Science, Kyoto University, Kyoto 606-01, Japan

Rafael Garcia-Molina‡
Departamento de Física, Universidad de Murcia, Apartado 4021, E-30080 Murcia, Spain

Isabel Abril
Departament de Física Aplicada, Universitat d'Alacant, Apartat 99, E-03080 Alacant, Spain
(Received 1 December 1999; published 9 June 2000)

Energy losses of fragment protons from 0.2- and 0.5-MeV/amu H_2^+ were measured at transmission through amorphous carbon foils of thickness less than 25 $\mu g/cm^2$. The energy losses of randomly oriented fragment protons and those of the fragment protons aligned in the direction of motion show how the spatial correlation of the protons affects the energy loss. We use the dielectric formalism to calculate the stopping power of amorphous carbon for two spatially correlated protons and compare with the experimental energy-loss data. We conclude that higher energies or thinner foils are necessary to understand the anomalous energy loss of aligned proton pairs.

PACS number(s): 34.50.Bw, 36.40.−c

I. INTRODUCTION

The behavior of fast charged particles moving through solids is an important subject, since its study offers both basic and applied possibilities to improve our understanding of the nature of matter and allows a controlled modification of the properties of materials. Recent studies [1,2] have made clear the role played by the collective response of valence electrons of the solid in the energy loss of fast charged particles moving through it. This response is called *polarization wake* and represents electron density oscillations trailing behind the charged particle [1,3]. This wake affects not only the motion of the particle that creates it, but also the motion of nearby charged particles [4].

In the pioneering study of the energy loss of fragment protons that result from the dissociation of H_2^+ and H_3^+ in carbon and gold foils, Brandt *et al.* [5] showed that the ratio of the energy loss of a cluster of protons to the sum of the energy losses of the corresponding isolated components is larger than 1. The result that the energy-loss ratio is different from unity was ascribed to the interference of the polarization wakes created by the fragments, which modify the retarding force acting on the protons of a cluster; this is referred to as *vicinage effects*. Since this study, many experimental and theoretical works have been published on the energy loss of fragments of molecular ions [6–17].

Theoretical studies have shown that the energy loss of a pair of correlated ions depends on their velocity as well as on the length and orientation of the internuclear axis of the pair with respect to the direction of motion. Steuer *et al.* [9] measured the energy loss of the fragments resulting from the dissociation of diatomic molecular ions with their internuclear axes parallel to the beam direction, where a sizeable variation in energy loss is expected.

Determinations of the energy loss of fragment ions in thin foils, except for the study by Brandt *et al.* [5], have so far been done through the measurements of the energies of emerging individual fragment ions. In the present investigation we have arranged an experimental setup where only the energy losses of proton pairs are detected. After transmission of the fragments dissociated from H_2^+ ions through amorphous carbon foils, energy-loss ratios are measured for the proton pairs exiting the foil with the internuclear axis oriented randomly, or parallel, to the direction of motion. For comparison with the experimental energy-loss ratios, we have calculated the stopping power of amorphous carbon for spatially correlated protons, using the dielectric formalism [18] to describe the electronic excitations in the stopping medium and taking into account the time evolution of the internuclear separation due to Coulomb repulsion between both protons.

II. EXPERIMENTAL SETUP

A narrowly collimated beam of H_2^+ or H^+ ions with energies 0.2 and 0.5 MeV/amu from the 4-MV Van de Graaff accelerator of Kyoto University was introduced in a scattering chamber at high vacuum conditions, where a movable target ladder was mounted. Self-supporting amorphous carbon foils of thicknesses ranging from 2 $\mu g/cm^2$ to 25 $\mu g/cm^2$ were mounted on the target ladder holding seven foils. The mass density of the target was 1.65 g/cm^3 and the foil thicknesses were determined comparing the measured energy losses for protons at 0.2 MeV and 0.5 MeV with the stopping power data compiled by Andersen and Ziegler [19]. The diameter of the beam was less than 10 μm, the irradiation was done at several positions per each foil, and the

*Present address: Department of Physics, Osaka Kyoiku University, Kashiwara, Osaka 582, Japan.
†Present address: HSTD Tester Business, Hewlett-Packard Japan Ltd., 9-1, Takakura-Cho, Hachioji-Shi, Tokyo 192-8510, Japan.
‡Corresponding author.

measured thickness was averaged. We checked that the differences in measured thicknesses, due both to the inhomogeneities of the foils and the calibration with two proton energies, were within 5%. The effect of impurities on the target is very small, a few percentage points in our experiment [20].

The ions transmitted through each one of the foils on the ladder were detected by either of two solid-state detectors (SSD, PD25-10-500, and PD25-10-100 AM, Camberra Industries, Inc.) placed at 5 cm and 278 cm downstream from the target. The former SSD, which we call U-SSD hereafter, accepted ions scattered within angles less than 3.2°, and the latter one, which we call D-SSD, did the same with ions scattered within angles less than 0.04°.

The angular deflections of the fragment H^+ ions resulting from the Coulomb explosion of H_2^+ ions in free space were less than 0.8° for the slowest H_2^+ ions used in the experiment; thus the acceptance half angle of the U-SSD was wide enough to detect almost all the pairs of H^+ ions formed in the foil; i.e., the randomly oriented fragment pairs (*random pairs*) were detected. On the other hand, the D-SSD could accept only the fragment pairs with their internuclear axes aligned parallel to the direction of motion; we will refer to these pairs as *aligned pairs* in the following. To eliminate H_2^+ ions that could be transmitted through the thinner foils or formed by recombination of protons at foil exit, a magnetic charge-state separator was installed in front of the D-SSD; in any case, these H_2^+ would have a negligible contribution to the loss, as its fraction is rather small [21]. In the energy spectrum obtained from the D-SSD, the yield of fragment pairs is small compared with the yield of isolated protons. To avoid the random pulse pile-up of the isolated protons, we measured the energy spectra of proton pairs at a counting rate less than about 100 pulses/s. The energy spectra of the incident H_2^+ ions were measured with the two SSD's.

III. EXPERIMENTAL RESULTS

The mean electric pulse height produced by the pairs of protons was almost twice as large as that of single protons of the same velocity, and almost all the detected pulses at the U-SSD were due to fragment pairs. In the energy spectrum obtained with the D-SSD, a peak due to isolated protons was observed besides the peak due to aligned pairs that we wanted to measure. These isolated protons had lost the memory of their initial molecular orientation and their partner protons as the result of multiple small-angle scattering in the foil. In Fig. 1 we show the thickness dependence of the ratio of the fraction of aligned pairs to the isolated proton fraction transmitted through the foil for the case of 0.5 MeV/amu H_2^+. Even at the thinnest foil used here, the fraction of the aligned pairs was only about 3%, showing that the correlated motion of the fragment pair is considerably disturbed by the multiple small-angle scattering.

After the correction of energy loss in the surface dead layer (about 50 nm equivalent thickness of Si) of the SSD's, the pulse heights were converted into energies. The energy resolution of the SSD's was 10 keV, however the peak of the

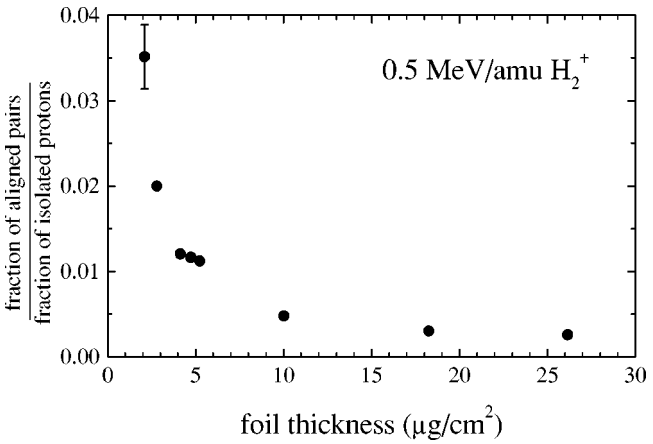

FIG. 1. Thickness dependence of the ratio of the fraction of aligned pairs to the fraction of isolated protons transmitted through the amorphous carbon foil. The energy of the H_2^+ beam was 0.5 MeV/amu.

energy spectrum could be fitted to a Gaussian distribution and the most probable energy at the peak was determined with an accuracy of 0.1 keV.

From the difference of the peak energy E of the incident H_2^+ ions and the peak energy $E_f(z)$ of the pair of protons transmitted through a foil of thickness z, the most probable energy loss of the fragment pairs was determined as $\Delta E(z) = E - E_f(z)$. Energy losses of 0.2 and 0.5 MeV/amu H^+ ions were also measured for comparison with the losses of the fragments. The dependence of the most probable energy loss of random pairs (ΔE_R), aligned pairs (ΔE_A), and isolated protons (ΔE_p), on the thickness z of carbon foil at the transmission of 0.2 and 0.5 MeV/amu H_2^+ and H^+ ions is shown in Figs. 2(a) and 2(b), respectively. The ratios between the energy losses of proton pairs and isolated protons, $\Delta E_j(z)/2\Delta E_p(z)$ ($j = A, R$, where A and R stand for aligned

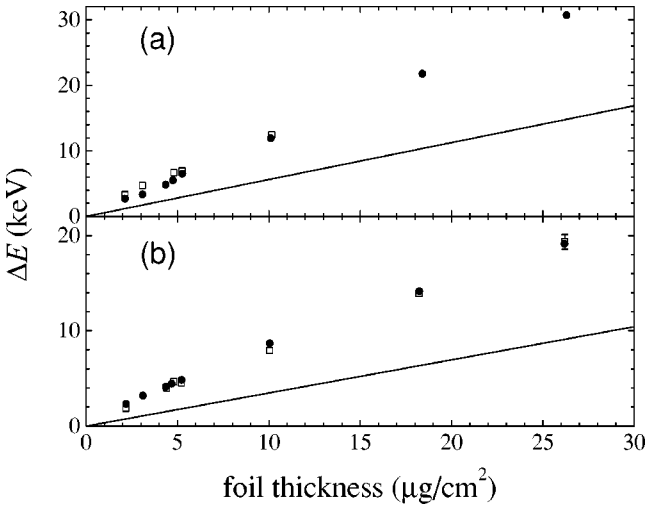

FIG. 2. Thickness dependence of the most probable energy losses of random pairs (● ΔE_R), aligned pairs (□ ΔE_A), and isolated protons (— ΔE_p) at the transmission of (a) 0.2 MeV/amu and (b) 0.5 MeV/amu H_2^+ and H^+ ions through amorphous carbon foils.

and random, respectively), will characterize the vicinage effects of the fragments dissociated from H_2^+ ions and transmitted through the carbon foils.

IV. THEORY

The mean energy loss of a spatially correlated pair of ions differs from the sum of the energy losses that would be experienced by the individual ions. This vicinage effect depends on the molecular velocity and the orientation and length of the internuclear vector. In what follows we shall consider only the electronic energy loss since this is the principal mechanism at high velocities. Atomic units [22] will be used throughout these calculations.

The stopping power S_p for a proton moving with velocity v through a medium characterized by a dielectric function $\varepsilon(q,\omega)$ is expressed in the dielectric formalism as

$$S_p=\frac{2}{\pi v^2}\int_0^\infty \frac{dq}{q}\int_0^{qv} d\omega\,\omega\,\mathrm{Im}\left[\frac{-1}{\varepsilon(q,\omega)}\right], \tag{1}$$

where q and ω are the momentum and energy transferred to the electronic excitations of the stopping medium. Taking into account the correlated motion of the two protons resulting from the dissociation of the H_2^+ ion, the electronic stopping power for the pair of protons moving with velocity v is given by [14]

$$S_{\mathrm{pair}}(r,\theta)=2\,[1+I(r,\theta)]\,S_p, \tag{2}$$

where $I(r,\theta)$ is the vicinage function, S_p is the stopping power for a single proton, given by Eq. (1), r is the internuclear distance, and θ is the angle between the internuclear vector and the direction of motion of the pair.

The vicinage function $I(r,\theta)$ measures the collective effects that appear in the stopping power for the correlated proton pair and it can be written as [14]

$$I(r,\theta)=\frac{2}{\pi v^2 S_p}\int_0^\infty \frac{dq}{q}\int_0^{qv} d\omega\,\omega\,\mathrm{Im}\left[\frac{-1}{\varepsilon(q,\omega)}\right] \times\cos\left(\frac{r\omega\cos\theta}{v}\right)J_0(r\sin\theta\sqrt{q^2-\omega^2/v^2}), \tag{3}$$

where $J_0(\cdots)$ is the Bessel function of the first kind. For the case of random pairs, the vicinage function only depends on the internuclear distance r and it becomes

$$I_R(r)=\langle I(r,\theta)\rangle_\theta =\frac{2}{\pi v^2 S_p}\int_0^\infty \frac{dq}{q}\,\frac{\sin(qr)}{qr}\int_0^{qv} d\omega\,\omega\,\mathrm{Im}\left[\frac{-1}{\varepsilon(q,\omega)}\right], \tag{4}$$

where $\langle\cdots\rangle_\theta$ denotes the angular average. For a pair of protons oriented in the direction of motion, i.e., for the aligned pair, we have the vicinage function

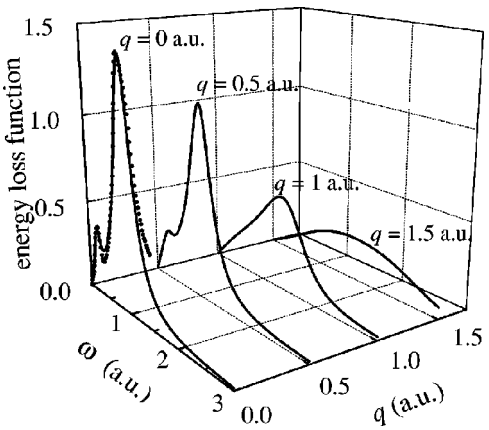

FIG. 3. Energy-loss function $\mathrm{Im}[-1/\varepsilon(q,\omega)]$ of amorphous carbon. The dots at $q=0$ show experimental data from Ref. [26]. The solid lines correspond to results obtained with Eq. (6), as described in the text.

$$I_A(r)=I(r,0) =\frac{2}{\pi v^2 S_p}\int_0^\infty \frac{dq}{q}\int_0^{qv} d\omega\,\omega\,\mathrm{Im}\left[\frac{-1}{\varepsilon(q,\omega)}\right]\cos\left(\frac{r\omega}{v}\right). \tag{5}$$

In order to evaluate the stopping power using Eqs. (2), (4), and (5), it is necessary to specify the dielectric function $\varepsilon(q,\omega)$ of the amorphous carbon foils; we model the dielectric properties of the target by a sum of two Mermin-type energy-loss functions [18,23],

$$\mathrm{Im}\left[\frac{-1}{\varepsilon(q,\omega)}\right]=\sum_{i=1}^{2} A_i\,\mathrm{Im}\left[\frac{-1}{\varepsilon_M(q,\omega;\omega_i,\gamma_i)}\right], \tag{6}$$

where ε_M is the Mermin dielectric function [24] and ω_i and γ_i are plasmon energy and damping, respectively, which are related to the location and width of the peaks in the energy-loss function $\mathrm{Im}[-1/\varepsilon(q=0,\omega)]$. Mermin's dielectric function is a generalization of Lindhard's dielectric function for a free-electron gas [25], but it takes into account the finite plasmon lifetime and preserves the local particle number. We fitted the experimental energy-loss function for amorphous carbon, taken from Ref. [26], with the expression (6) at $q=0$, using A_i, ω_i and γ_i as the fitting parameters; the coefficients A_i in Eq. (6) were calculated imposing sum rules to fit to the number of valence electrons in carbon. Using the set of parameters $A_1=0.2363$, $\omega_1=0.23$ a.u., $\gamma_1=0.21$ a.u., $A_2=0.7088$, $\omega_2=0.94$ a.u., and $\gamma_2=0.49$ a.u., we reproduce the two broad peaks at $\sim$0.2 a.u. and $\sim$0.9 a.u., which correspond to the collective excitations of π and $\sigma+\pi$ electrons in carbon, respectively. In Fig. 3 we show the evolution of the energy-loss function $\mathrm{Im}[-1/\varepsilon(q,\omega)]$ of amorphous carbon as a function of the transferred energy ω and momentum q. The dots represent the experimental data from Ref. [26] at $q=0$. It is appreciated from Fig. 3 that the peak structure at $q=0$ disappears as q increases, which means that the collective excitations decay to single excitations at q

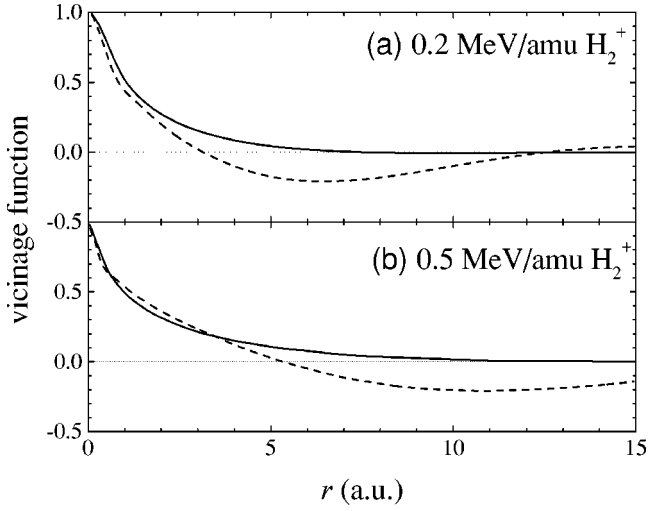

FIG. 4. Vicinage functions for random pairs (—) and for aligned pairs (- - -) in amorphous carbon. (a) 0.2 MeV/amu H_2^+ and (b) 0.5 MeV/amu H_2^+.

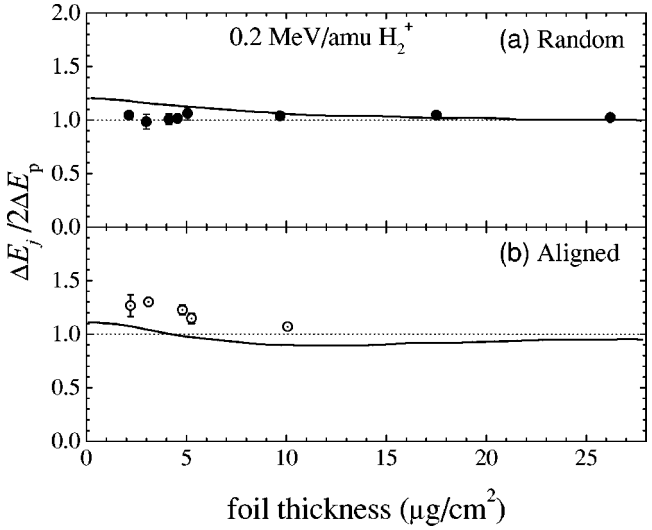

FIG. 5. Comparison of the experimental (symbols) and calculated (solid lines) energy-loss ratios of (a) random pairs, $\Delta E_R/2\Delta E_p$, and (b) aligned pairs, $\Delta E_A/2\Delta E_p$, at the transmission of 0.2 MeV/amu H_2^+ through amorphous carbon foils, plotted as a function of the foil thickness.

>0, a behavior that is well reproduced by our model when compared with available experimental data [27].

Equations (4) and (5) are calculated with the energy-loss function shown in Fig. 3. In Fig. 4 we show the vicinage functions for random pairs and for aligned pairs, as a function of the internuclear distance, for the case of 0.2 and 0.5 MeV/amu H_2^+ ions. The vicinage function $I_R(r)$ for random pairs decreases monotonically as r increases. Figure 4(a), corresponding to 0.2 MeV/amu H_2^+, shows that $I_R(r)$ is practically zero at about $r\sim 7$ a.u. On the other hand, $I_A(r)$ decreases rapidly with increasing distance r and becomes negative at $r\gtrsim 3$ a.u. It is negative even at $r\gtrsim 10$ a.u. and approaches to zero at larger r, where the interference effects gradually vanish. The positive and negative values of the vicinage function $I_A(r)$ come from the position of the trailing proton relative to the leading one, where the force due to the wake of the leading proton may be repulsive or attractive on the trailing proton. Similar characteristic features can be seen in the vicinage function for the case of 0.5 MeV/amu H_2^+ ions, shown in Fig. 4(b), but now the negative interference effects appear for larger internuclear distances.

After the H_2^+ ion enters the target it loses its binding electron in the first few atomic layers and then it moves through the target as a pair of correlated protons undergoing mutual repulsion. Therefore, the internuclear separation r increases as the pair of protons moves deeper in the target. Using a screened Coulomb potential $V(r)=r^{-1}\exp(-r/a)$ [28], where $a=v/\omega_{\rm pl}$ is the screening length and $\omega_{\rm pl}=0.94$ a.u. is the largest plasmon energy of the amorphous carbon target, we have obtained the time-dependent internuclear separation $r(t)$, assuming an initial value r_0 at its entrance of the target surface. It is worth noting that in the velocity regime which we are dealing with in this work, the final results of energy losses hardly change if we consider a pure Coulomb potential.

Equation (2) provides the stopping power of the target for a proton pair with a given internuclear separation, for the cases of random and aligned pairs. Taking into account that the internuclear separation increases as the proton pair penetrates the target, $r(t)$, and assuming that the velocity v is constant, the energy loss of the proton pair traversing a foil of thickness z is

$$\Delta E_j(z)=2vS_p\int_0^{z/v} dt\,[1+I_j(r(t))] \quad (j=R,A), \qquad (7)$$

where $I_R(r(t))$ and $I_A(r(t))$ are given by Eqs. (4) and (5), respectively. Finally the energy-loss ratio will be

$$\frac{\Delta E_j(z)}{2\Delta E_p(z)}=1+\frac{v}{z}\int_0^{z/v} dt\, I_j(r(t)) \quad (j=R,A). \qquad (8)$$

Using the vicinage functions depicted in Fig. 4, the ratios of energy losses, Eq. (8), for random and aligned pairs were calculated for 0.2 MeV/amu and 0.5 MeV/amu H_2^+ ions. This ratio characterizes the deviation from the energy-loss additivity of the individual noncorrelated protons resulting from the dissociation of a molecule, and indicates the interference effects in the energy loss due to the correlated motion of two protons in an amorphous carbon foil.

From the widths of the peaks of the energy spectra of the fragment protons, we found that the internuclear separation of H_2^+ had a rather broad distribution, as noted by Brandt *et al.* [5]. In order to check the effect of the initial internuclear separation on the energy loss ratio, we calculated this ratio using a mean value of $r_0=1.25$ Å and also taking into account the initial distribution of the distances, but the energy-loss ratios were practically the same in both cases for the range of thicknesses studied in the present work.

V. DISCUSSION AND CONCLUSIONS

In Figs. 5 and 6 we have depicted the energy-loss ratios for random and aligned pairs for the case of 0.2 and 0.5

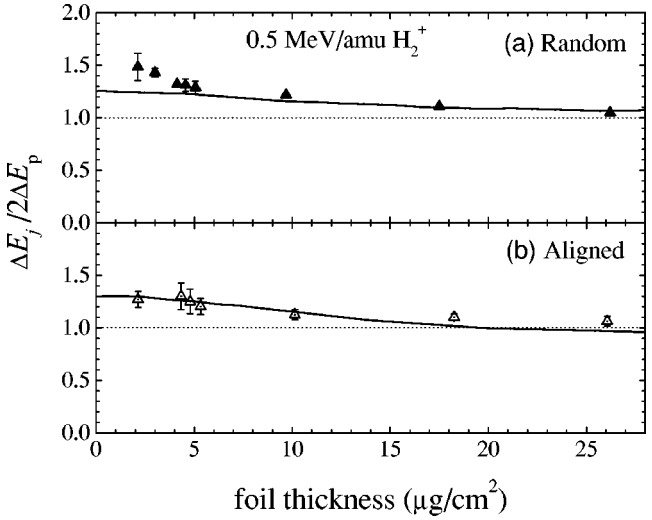

FIG. 6. Comparison of the experimental (symbols) and calculated (solid lines) energy-loss ratios of (a) random pairs, $\Delta E_R/2\Delta E_p$, and (b) aligned pairs, $\Delta E_A/2\Delta E_p$, at the transmission of 0.5 MeV/amu H_2^+ through amorphous carbon foils, plotted as a function of the foil thickness.

MeV/amu H_2^+ ions, as a function of the carbon foil thickness expressed in μg/cm^2. The experimental energy-loss ratios (represented by symbols) were derived from the data in Fig. 2 and are compared with the calculated ones (shown by solid lines). The theoretical ratios for random pairs are always larger than unity for both energies. The ratios for aligned pairs decrease more rapidly than those for random pairs, and become less than unity, after which they approach unity for larger thicknesses.

It must be noted, however, that all the measured ratios for aligned pairs are larger than unity, while the theory predicts ratios smaller than unity at larger foil thicknesses. This discrepancy may be related to the multiple small-angle scattering in the foils: Even at the thinnest foil and higher energy used in the experiment, the detected aligned pairs are about 3% of the total detected ions in the forward direction, as was shown in Fig. 1. This indicates that, despite the tendency to alignment due to the wake potential, the correlated motion of a pair of protons is effectively disturbed by the multiple small-angle scattering and that the direction of the initial internuclear vector is hardly preserved in the foil transmitted pairs. We may interpret this energy loss of the nominal aligned pairs as being the result of an average over a small angular region; thus the energy-loss ratio becomes similar to that of random pairs as the foil thickness increases.

Deviations of the energy-loss ratios of the aligned pairs of 0.2 MeV/amu H_2^+ from the theoretical curve are larger at the thinnest foils. The deviations come from the large energy losses of the aligned pairs and are supposed to be related to the mechanism of energy-loss measurement used in the experiment. In the present experimental setup, we expected that the protons of a pair hit the SSD simultaneously and that the SSD generates a single electric pulse. This was realized in the U-SSD, where the maximum interval of two arriving protons of a pair was about 90 ps. In the D-SSD, however, the trailing proton of the aligned pair originated from a 0.2 MeV/amu H_2^+ hits the D-SSD about 5.2 ns after the hit of the leading proton. This interval is comparable to the rise times of the electric pulse generated by an isolated proton in the semiconductor detector and of the output voltage signal of the preamplifier. The delayed proton signal may overlap the preceding proton signal to give a signal that is slightly smaller in height than the signal of the proton pair hitting the SSD simultaneously. This effect was not observed for aligned pairs of 0.5 MeV/amu H_2^+, where the corresponding interval is 3 ns.

The energy-loss ratio increases with the projectile energy both for random and aligned proton pairs and goes to unity at larger foil thickness. This behavior is because the interference effects spread at larger internuclear distances as the energy increases. This tendency is followed both by the calculations and by the experimental data.

We conclude that, in the range of energies and thicknesses studied in this work, there are no significant experimental differences for the energy-loss ratio of aligned and random pairs; the main discrepancies appear for the thinner foils, which are the more difficult to be properly characterized. It is desirable to use higher-energy H_2^+ ions or thinner target foils to detect the anomalous energy loss of aligned proton pairs. The effects of multiple small-angle scattering of fragment pairs can be made smaller at the above-mentioned experimental conditions.

ACKNOWLEDGMENTS

We are grateful to the members of the Department of Nuclear Engineering for the use of the 4-MV Van de Graaff accelerator of Kyoto University. Financial support provided to R.G.-M. and I.A. from the Spanish Dirección General de Enseñanza Superior (Project No. PB96-1118) and the Generalitat Valenciana (Project No. GV99-54-1-01) is acknowledged.

[1] P. M. Echenique, F. Flores, and R. H. Ritchie, in *Solid State Physics*, edited by H. Ehrenreich and D. Turnbull (Academic, New York, 1990), Vol. 43, p. 229.

[2] Proceedings of the Conference on Polyatomic Ion Impact on Solids and Related Phenomena, Saint Malo, 1993, edited by H. Andersen and L. E. Rehn [Nucl. Instrum. Methods Phys. Res. B **88**, 1 (1994)].

[3] Z. Vager and D. S. Gemmell, Phys. Rev. Lett. **37**, 1352 (1976).

[4] D. S. Gemmell, J. Remilleux, J.-C. Poizat, M. J. Gaillard, R. E. Holland, and Z. Vager, Phys. Rev. Lett. **34**, 1420 (1975).

[5] W. Brandt, A. Ratkowski, and R. H. Ritchie, Phys. Rev. Lett. **33**, 1325 (1974).

[6] J. W. Tape, W. M. Gibson, J. Remillieux, R. Laubert, and H. E. Wegner, Nucl. Instrum. Methods **132**, 75 (1976).

[7] J. C. Eckardt, G. Lantschner, N. R. Arista, and R. A. Baragiola, J. Phys. C **11**, L851 (1978).

[8] R. Levi-Setti, K. Lam, and T. R. Fox, Nucl. Instrum. Methods **194**, 281 (1982).
[9] M. F. Steuer, D. S. Gemmell, E. P. Kanter, and B. J. Zabransky, IEEE Trans. Nucl. Sci. **NS-30**, 1069 (1983).
[10] E. Ray, R. Kirsch, H. H. Mikkelsen, J. C. Poizat, and J. Remillieux, Nucl. Instrum. Methods Phys. Res. B **69**, 133 (1992).
[11] N. R. Arista and V. H. Ponce, J. Phys. C **8**, Ll88 (1975).
[12] A. R. Nyaiesh, W. Steckelmacher, and M. W. Lucas, J. Phys. C **11**, 2917 (1978).
[13] J. Steinbeck and K. Dettmann, J. Phys. C **11**, 2907 (1978).
[14] N. R. Arista, Phys. Rev. B **18**, 1 (1978).
[15] G. Basbas and R. H. Ritchie, Phys. Rev. A **25**, 1943 (1982).
[16] J. C. Ashley and P. M. Echenique, Phys. Rev. B **35**, 1521 (1987).
[17] J. Steinbeck, M. W. Lucas, J. Kemmler, and K.-O. Groeneveld, Nucl. Instrum. Methods Phys. Res. B **48**, 51 (1990).
[18] I. Abril, R. Garcia-Molina, C. D. Denton, J. Pérez-Pérez, and N. R. Arista, Phys. Rev. A **58**, 357 (1998).
[19] H. H. Andersen and J. F. Ziegler, *Hydrogen Stopping Powers and Ranges in all Elements* (Pergamon, New York, 1977).
[20] H. Ogawa, N. Sakamoto, I. Katayama, Y. Haruyama, M. Saito, K. Yoshida, M. Tosaki, Y. Susuki, and K. Kimura, Nucl. Instrum. Methods Phys. Res. B **132**, 36 (1997).
[21] N. Cue, N. V. de Castro-Faria, M. J. Gaillard, J.-C. Poizat, J. Remillieux, D. S. Gemmell, and I. Pleaser, Phys. Rev. Lett. **45**, 613 (1980).
[22] Atomic units are defined by the condition $m_e = e = \hbar = 1$, where m_e is the mass of the electron and e is the elementary charge.
[23] I. Abril, R. Garcia-Molina, and N. R. Arista, Nucl. Instrum. Methods Phys. Res. B **90**, 72 (1994).
[24] N. D. Mermin, Phys. Rev. B **1**, 2362 (1970).
[25] J. Lindhard, Mat. Fys. Medd. K. Dan. Vidensk. Selsk. **28**, No. 8 (1954).
[26] J. Cazaux and P. Gramari, J. Phys. (Paris) **38**, L133 (1977).
[27] D. J. Planes, R. Garcia-Molina, I. Abril, and N. R. Arista, J. Electron Spectrosc. Relat. Phenom. **82**, 23 (1996).
[28] W. Brandt, in *Atomic Collisions in Solids*, edited by S. Datz, B. R. Appleton, and C. D. Moak (Plenum, New York, 1975), p. 261.